Microwave Review
July 2026, Vol. 32, No. 1, pp. 20-27
DOI: 10.18485/mtts_mr.2026.32.1.4

Reliability of the Digital Models of Open/Short-Circuited Coupled-Line Branch-Line Structures

Biljana P. Stošić[1] and Marin Nedelchev[2]

Abstract – **This paper introduces the reliability of digital models for coupled-line branch-line structures containing open-circuited or open- and short-circuited parallel-coupled sections, widely used in radio-frequency and microwave systems. The study focuses on evaluating the accuracy of the model in replicating the structure's frequency-dependent behavior using digital signal processing techniques, allowing for efficient simulation and analysis in time-domain environments. The effects of coupling, open-circuit and short-circuit terminations, and line impedance are incorporated to ensure realistic performance representation. Validation through simulation confirms the model's effectiveness in capturing the essential characteristics of the physical structure.**

Keywords – **Wave digital approach, Four-port structure, Transmission lines, Branch-line coupler, Parallel-coupled lines.**

I. INTRODUCTION

The standard structure of a branch-line coupler works on the transmission line theory, where power is split or combined depending on the impedance, length of the lines of the branches and the interaction between the ports. However, standard single-section designs are inherently narrowband due to the frequency dependence of quarter-wavelength transmission lines. Wideband variants have been developed using multi-section or coupled-line configurations to extend the coupling and isolation responses over a wider frequency range, often extending the fractional bandwidth to more than 30–50% of the center frequency. The studies given in [1-3] highlight various innovative approaches to enhancing the performance and compactness of wideband branch-line couplers using coupled lines, catering to the growing demands of modern microwave and radio-frequency (RF) applications.

Over the last two decades, the wave digital (WD) approach — based on A. Fettweis's wave digital filter theory [4, 5] — has been widely used to model physical systems using wave variables (incident and reflected waves), offering advantages for various circuit structures. Extensive literature exists on WD-based modelling [6-13], with some models validated against full-wave simulations using equivalent circuit representations [14].

The paper details in derivation of WD models for wideband branch-line couplers with open-circuited and open/short-circuited parallel-coupled line sections using admittance (*J*-) and impedance (*K*-) inverter equivalent circuits, as well as a systematic reliability assessment comparing WD results to ADS and HFSS across different coupling levels and impedance values. The paper demonstrates that WD models maintain FBW accuracy within ~1–2% for the studied configurations.

Structure of the paper is as follows. Section II provides a short explanation of the WD modelling approach. The next Section III deals with the methodology for converting parallel-coupled line sections into wave digital models. The actual branch-line coupler structures are introduced in Section IV, including their layouts, physical dimensions, and electrical characteristics. This section also includes simulation results comparing the wave digital model to commercial simulation tool. Section V evaluates the reliability and accuracy of the coupler WD models under different conditions. It investigates how the models behave with variations in line impedance and frequency. The paper Section VI concludes by summarizing the findings, emphasizing the advantages of using the wave digital approach for modelling complex coupled-line structures.

II. WD MODEL OVERVIEW

The WD approach is a technique used to convert analog and lumped-element circuits into a digital representation [10, 13-15]. In this context, it involves transforming the branch-line coupler, which is typically represented by reactive elements (inductors and capacitors), into a system of digital wave variables that can be processed by digital signal processing (DSP) algorithms.

In order to apply WD approach [15] to a branch-line coupler, the following steps are to be taken:

- Replacing circuit elements with digital blocks: This involves replacing the transmission lines with wave digital elements that represent the behavior of the analog transmission line in a digital context.
- Using wave variables: The WD model uses wave variables (which represent the traveling waves on transmission lines) in place of the voltages and currents in the original.
- Impedance matching: Impedance matching is an important consideration in a branch-line coupler. In the WD model, digital impedances are chosen so that the wave variables accurately simulate the power division behavior of the coupler. The impedance at each port of the branch-line coupler is matched to the digital wave variables.

Article history: Received April 09, 2026; Accepted May 18, 2026. This paper is an expanded version of the article "Reliability of the Digital Model of an Open-Circuited Coupled-Line Branch-Line Structure," presented at 60th International Scientific Conference on Information, Communication and Energy Systems and Technologies, Ohrid, North Macedonia, June 26–28, 2025. [DOI: 10.1109/ICEST66328.2025.11098325].

[1]Biljana P. Stošić is with University of Niš, Faculty of Electronic Engineering, Aleksandra Medvedeva 4, 18000 Niš, Serbia, E-mail: biljana.stosic@elfak.ni.ac.rs

[2]Marin Nedelchev is with Technical University of Sofia, Faculty of Telecommunications, 1000, 8 Kl. Ohridski Blvd, Sofia, Bulgaria, E-mail: mnedelchev@tu-sofia.bg

- Port connecting: The ports of the branch-line coupler are connected through WD components such that the input wave is distributed to the output ports with specific amplitude and phase relations according to the branch-line coupler design.
- Simulating and analyzing WD model: Once the model is set up, various analyses can be performed, such as frequency response (through Fourier transforms), and time-domain responses.

III. Modelling Parallel-Coupled Sections Using Wave Digital Approach

To facilitate the analysis of the wideband branch-line couplers, particularly within the WD framework, the parallel-coupled line sections are transformed into an equivalent network using transmission lines and admittance/impedance inverter. A mathematical foundation for structural transitions is provided here.

A. Equivalent Circuit Representation of an Open-Circuited Parallel-Coupled Line Section

Based on common microwave engineering theory (specifically as presented in textbooks like [16, 17]), an open-circuited parallel-coupled line section (typically quarter-wavelength long, $\lambda/4$, at the center frequency) can be modeled using an admittance inverter (*J*-inverter). This coupled line section, Fig. 1*a* (typically ports 2 and 3 open, inputs at 1 and 4), is equivalent to a network consisting of an admittance inverter ($J, -90^o$) connected between two transmission line sections, as shown in Fig. 1*b* [18-21]. The transmission line sections on either side have a characteristic admittance Y_0 (or impedance $Z_0 = 1/Y_0$, often chosen to be the system impedance) and an electrical length of θ (which is 90^o or $\pi/2$ at the center frequency f_0, corresponding to the physical λ/4 length).

(a) (b)

Fig. 1. (a) An open-circuited parallel-coupled section, (b) Its equivalent circuit

The *J*-inverter value required to model the coupled section is:

$$J = \frac{Z_{0e} - Z_{0o}}{2 \cdot Z_0^2} = \frac{Y_{0o} - Y_{0e}}{2}. \qquad (1)$$

The characteristic impedance of transmission line is calculated as $Z_0 = \sqrt{Z_{0e} \cdot Z_{0o}}$, where Z_{0e} and Z_{0o} represent the even and odd mode characteristic impedance, respectively.

Furthermore, having in mind that admittance inverter represents an idealized two-port device operating electrically like a quarter-wave lossless transmission line of characteristic impedance $1/J$, its *ABCD* parameters are obtained and then converted into *S*-parameters [18].

Namely, physical coupling between transmission line sections can be approximated using a *J*-inverter (the admittance inverter emulates the coupling). This simplifies analysis by converting a distributed structure (coupled lines) into a modular form. In general, a digital circuit that represents the wave digital counterpart of the equivalent circuit shown in Fig. 1*b* is obtained and shown in Fig. 3. This circuit emulates the time-delay and phase-shifting characteristics of the physical coupled line section. Proper impedance matching in a WD model is critical for preventing reflections, and port values of the *J* - inverter model must match the characteristic impedance of the transmission lines.

B. Equivalent Circuit Representation of a Short-Circuited Parallel-Coupled Line Section

When ports on opposite ends of a parallel-coupled line section (of quarter-wavelength λ/4 at center frequency) are short-circuited, the resulting network has a different frequency response and equivalent model compared to the open-circuited version. While the open-circuited section is fundamentally a bandpass element, the short-circuited section acts as a bandstop (or notch) element. Specifically, at the center frequency (f_0, where length is λ/4), the short circuits are transformed into open circuits at the input ports, creating a transmission zero and providing high attenuation.

(a) (b)

Fig. 2. (a) A short-circuited parallel-coupled line section, (b) Its equivalent circuit

Just as the open-circuited section is modeled by a *J*-inverter between lines, the short-circuited parallel-coupled section defined by its even-mode and odd-mode characteristic impedances and electrical length θ can be modeled as a *K*-inverter (impedance inverter) between two transmission line sections of length θ. In this equivalent model, the coupling effect is captured by the *K* parameter, while the physical lines on either side account for the phase shift and the transformation of the short circuit. This approach, based on the established synthesis techniques by Matthaei [17], allows for a simplified two-port representation of the complex four-port coupled structure.

To determine the *K*-inverter value required to model a short-circuited parallel-coupled line section, it is needed to relate the inverter impedance *K* to the even-mode (Z_{0e}) and odd-mode (Z_{0o}) characteristic impedances of the coupled lines. For a quarter-wavelength (λ/4) section, the *K* value is derived from the difference of these model impedances as:

$$K = \frac{Y_{0e} - Y_{0o}}{2 \cdot Y_0^2} = \frac{Z_{0e} - Z_{0o}}{2}. \qquad (2)$$

Furthermore, having in mind that the impedance inverter (*K*-inverter) represents an idealized two-port device operating electrically like a quarter-wave lossless transmission line of

characteristic impedance *K*, its parameters are obtained and then converted into S-parameters [18]. While the admittance inverter (*J*) is typically used to model shunt-type resonators in bandpass structures, the impedance inverter (*K*) is employed here to model the coupling within the short-circuited parallel-coupled line sections, effectively transforming the series-type resonances into the required frequency response.

C. Wave Digital Model of Parallel-Coupled Line Sections

These previously given representations of coupled line sections are particularly advantageous for the WD approach. By replacing the coupled lines with an equivalent inverter and a standard transmission line, the adaptors' port resistances at the circuit nodes can be defined more intuitively.

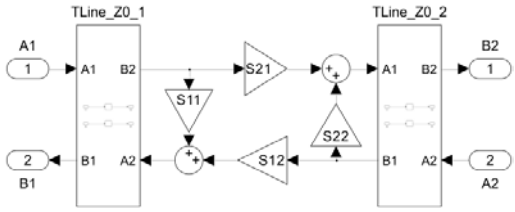

Fig. 3. Wave digital equivalent of a coupled-line section

Further, inverter is represented by its S-parameters and digital delay elements replace the transmission lines, as shown in Fig. 3. These delay elements simulate the propagation delay that the signal experiences as it travels along the line.

IV. Coupler Structural Description, Modelling and Simulation

In order to validate the proposed equivalent models and evaluate their performance, two distinct coupler configurations are analyzed: branch-line structure with open-circuited parallel-coupled sections utilizing admittance inverters to model the coupling between the sections, and branch-line structure with both open-circuited and short-circuited parallel-coupled sections utilizing both impedance and admittance inverters.

A. Branch-Line Structure with Open-Circuited Parallel-Coupled Sections

A conventional branch-line coupler with added open-circuited coupled-line sections at the input and output ports, Fig. 4, is an advanced RF/microwave component designed to enhance performance characteristics such as bandwidth and impedance matching. A schematic diagram of this structure can be found in the publication [22] by Arriola et al. The coupler is designed for upper C-band, at 5.9 GHz. Band 5.850–5.925 GHz represent common allocation for Intelligent Transportation Systems (ITS) and Vehicle-to-Everything (V2X) communications in many regions.

The conventional coupler structure typically consists of four transmission lines forming a square or rectangular layout, with each branch being a quarter-wavelength (λ/4) long at the center frequency f_0. This classical configuration achieves a 3 dB power split with a 90° phase difference between output ports. The open-circuit termination at the opposite ends of the coupled lines facilitates a bandpass response, where the electrical length θ = 90° ensures maximum power transfer and phase quadrature between the output ports.

At both the input and output ports, a coupled-line section is added, which is open-circuited at two ends. This section behaves as stub resonator or impedance transformer, introducing frequency-dependent reactance that can be used to tune the input/output matching or enhance isolation. The coupled lines are typically even/odd-mode impedance controlled, and their electrical length is chosen based on the desired frequency characteristics. The open-circuited end reflects signals back into the network, effectively contributing to the total impedance seen at the port and allowing fine control over bandwidth and return loss.

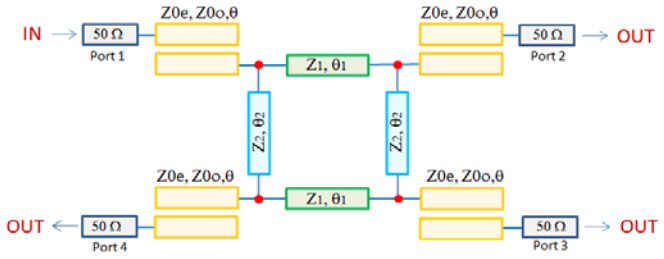

Fig. 4. Configuration of a coupler with open-circuited parallel-coupled sections

WD model of the coupler is given in Fig. 5 [23]. A three-port adaptor [15, 24] with assigned port resistances, as well as a network of adaptors and their positions and orientations are depicted in Fig. 6. The corresponding ADS (Advanced Design System from Keysight) schematic, which illustrates the electrical components and their interconnections, is shown in Fig. 7.

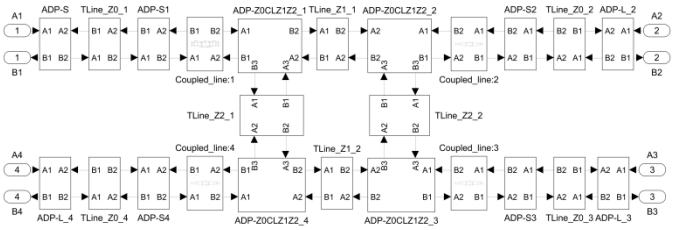

Fig. 5. WD model of a branch-line with open-circuited coupled-line structures. Input/output impedance matching is achieved via additional transmission lines Z_0

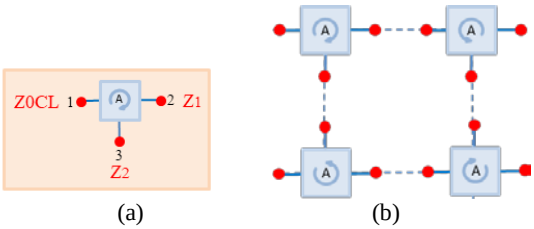

(a) (b)

Fig. 6. Branch-line structure with open-circuited parallel-coupled sections: (a) adaptor used in the WD model, (b) network of positions and orientations of adaptor A

Key metric such as frequency response (magnitude and phase of *S*-parameters) is analyzed to validate the model's performance. Frequency response estimated from WD and ADS models is presented in Fig. 8. In [22], measured results are presented for the coupler designed on Chukoh substrate, with a thickness of 0.5 mm and a relative permittivity of 2.6. As illustrated in the *S*-parameter plots, the design achieves a central operating frequency of 10 GHz, where it exhibits exceptional matching and isolation characteristics. It is evident that S_{21} and S_{31} are approximately −3 dB, indicating equal power split. Parameters S_{11} and S_{41} are less than −16 dB, indicating good isolation and matching of the coupler.

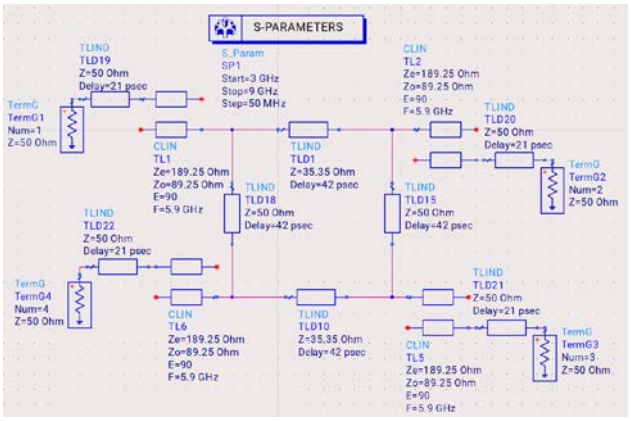

Fig. 7. ADS schematic of a branch-line coupler with open-circuited parallel-coupled sections (ADS model)

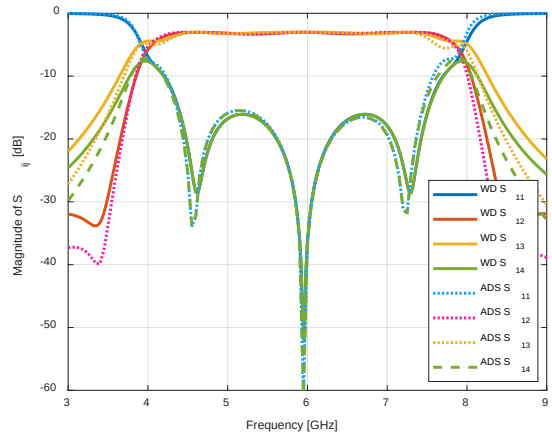

(a)

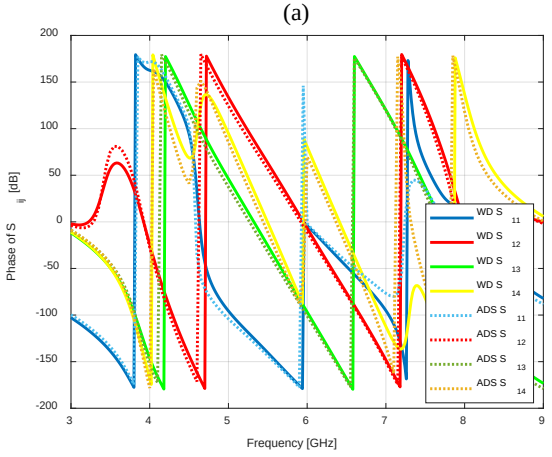

(b)

Fig. 8. Frequency response of a branch-line coupler with open-circuited parallel-coupled sections

B. Branch-Line Structure with Open- and Short-Circuited Parallel-Coupled Sections

In a standard design of branch-line coupler, the electrical length is typically λ/4 at the design center frequency. By using parallel-coupled sections (Z_{02} and Z_{03}) instead of simple transmission lines, the designer can manipulate the coupling coefficient and the matching bandwidth. This specific topology is often used in high-frequency applications (like the 10 GHz range) where tight coupling and broad bandwidth are required simultaneously. By short-circuiting the ports at opposite ends, the coupled line section is transformed into a dual resonant structure. This approach is particularly useful for achieving high-rejection bandstop characteristics or for synthesizing specific transmission zeros within the coupler's frequency response.

The schematic given in Fig. 9 illustrates a four-port microwave network that enhances standard branch-line coupler performance through the use of coupled-line sections [25]. The structure is symmetrical both horizontally and vertically, featuring a central rectangular "core" with coupled-line sections at each port.

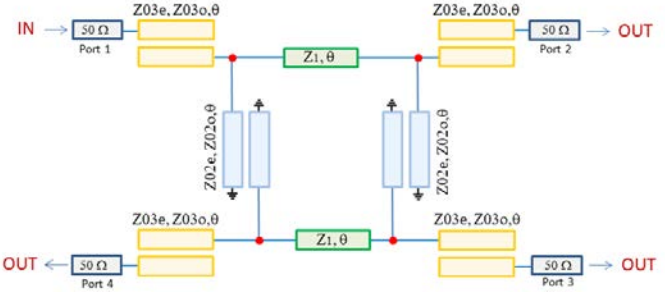

Fig. 9. Configuration of a coupler with open- and short-circuited parallel-coupled sections

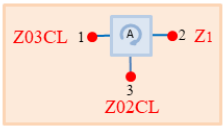

Fig. 10. Branch-line structure with open- and short-circuited parallel-coupled sections: Adaptor used in the WD model

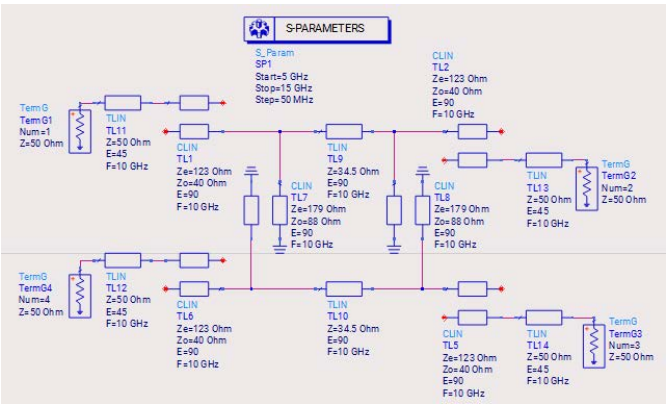

Fig. 11. ADS schematic of a branch-line coupler open- and short-circuited parallel-coupled sections (ADS model)

A three-port adaptor [15, 24] with assigned port resistances is depicted in Fig. 10. A network of adaptors and their positions and orientations are the same as the one given in Fig. 6*b*. An ADS schematic diagram that illustrates the electrical components and their interconnections within the circuit being analyzed are shown in Fig. 11. Figure 12 shows Ansys HFSS layout of the investigated coupler configuration (Substrate RO4350B: $h = 0.254$ mm and $\varepsilon_r = 3.65$, Line dimensions in mm: $w_{50} = 0.53$, $w_2 = 0.053$, $s_2 = 0.11$, $l_2 = 4.86$, $w_3 = 0.16$, $s_3 = 0.03$, $l_3 = 4.73$, and $w_1 = 0.94$ and $l_1 = 4.34$).

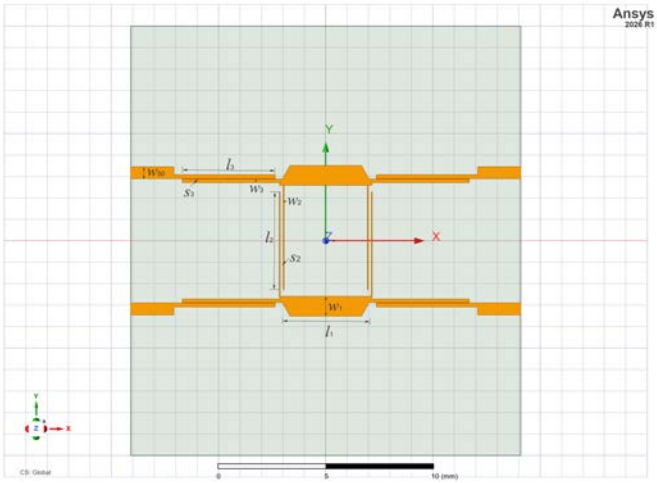

Fig. 12. HFSS layout of a branch-line coupler open- and short-circuited parallel-coupled sections

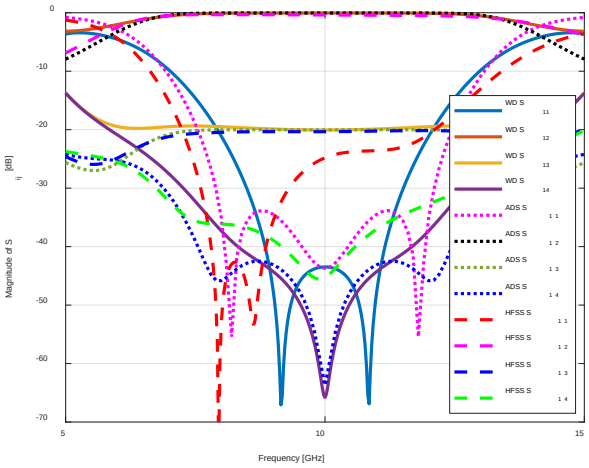

Fig. 13. Frequency response of a branch-line coupler with open-and short-circuited parallel-coupled sections

The provided plot (Fig. 13) shows the magnitude of *S*-parameters (dB) over a frequency range of 5 to 15 GHz for the coupler schematic discussed previously. It compares three simulation results: WD (solid lines), ADS (dotted lines) and HFSS (dashed lines). ADS and HFSS are the industry-standard softwares used to design and simulate high-frequency, high-speed electronic components, including antennas, RF/microwave circuits, IC packages, and PCBs. HFSS uses automated adaptive meshing to solve complex 3D electromagnetic field problems.

The flatness of the S_{13} curve indicates a very stable coupling coefficient over a fractional bandwidth of about 40%. Almost all parameters obtained from these three simulators, except S_{11} from HFSS, show excellent agreement regarding the center frequency, which is precisely at 10 GHz. At this point, the return loss (S_{11}) and isolation (S_{14}) show deep notches, characteristic of a well-matched and isolated design. The WD and ADS results show a very high level of correlation across the entire band. The notches of S_{14} at 10 GHz reach levels below –60 dB, following almost identical trajectories. The HFSS results (dashed red and green lines) follow the same general trend but exhibit a "shift" or different ripple behavior, particularly between 7 and 9 GHz. The HFSS S_{11} notch is also slightly less deep than the WD/ADS analytical models, which is typical as full-wave EM simulators (HFSS) account for parasitic effects and material losses that idealized circuit models might not fully capture.

The absolute bandwidth is calculated as:

$$BW = f_H - f_L\,, \tag{3}$$

and fractional bandwidth as:

$$FBW\,[\%] = \frac{f_H - f_L}{f_0}\cdot 100\,, \tag{4}$$

where f_H is the upper frequency and f_L is the lower frequency at defined value of –20 dB. If the bandwidth is define by $S_{11} < -20$ dB, the device operates effectively from approximately 7.95 GHz to 12.05 GHz, having fractional bandwidth of about 41%.

The plot analysis suggests that while the design is robust at the 10 GHz target, the WD modeling method may be utilizing different approximations compared to the ADS frequency-domain solver, leading to the differences seen in the wideband response.

V. Reliability of the Wave Digital Models

The reliability of a WD model depends on how well it represents the physical behavior of the analog system it models — in this case, the coupler circuit. This section investigates how developed WD models behave with variations in line impedance and frequency, as shown in Tables I and II. The goal is to determine whether the models maintain fidelity and stability under different scenarios.

A. Branch-line Coupler – Case I

The performance of the wideband branch-line coupler structure given in Fig. 4 was evaluated using both the WD modeling approach and ADS frequency-domain simulations, as tabulated in Table I.

Metrics such as absolute bandwidth (Eq. (3)) and fractional bandwidth (Eq. (4)) are discussed to support conclusions about the model's reliability. It is evident from these four coupler designs that WD model is able to estimate structure behavior accurately, with acceptable level of errors compared to commercial ADS software.

A comparative analysis of the FBW highlights the robustness of the design. Under a given return loss criterion, the WD model predicts a bandwidth which closely aligns with the ADS result for all investigated coupler structures. This

high degree of correlation (within a 1% margin) demonstrates that the WD modeling technique effectively captures the complex electromagnetic interactions of the coupled lines.

TABLE I
RELIABILITY OF WD MODELS OF COUPLER CASE I

Branch-line coupler specifications		Return Loss S_{11}		Isolation S_{14}	
		WD	**ADS**	**WD**	**ADS**
		< –16 dB		< –16 dB	
$f_0 = 5.9$ GHz, $Z_1 = 35.5\ \Omega$, $Z_2 = 50\ \Omega$, $Z_{0e} = 189.25\ \Omega$, $Z_{0o} = 89.25\ \Omega$	f_L [GHz]	4.4	4.38	4.4	4.38
	f_H [GHz]	7.5	7.42	7.5	7.42
	BW [GHz]	3.1	3.04	3.1	3.04
	FBW [%]	52.5	51.5	52.5	51.5
		WD	**ADS**	**WD**	**ADS**
		< –15 dB		< –20 dB	
$f_0 = 5.9$ GHz, $Z_1 = 43.3\ \Omega$, $Z_2 = 86.7\ \Omega$, $Z_{0e} = 189.25\ \Omega$, $Z_{0o} = 89.25\ \Omega$	f_L [GHz]	4.43	4.41	4.51	4.58
	f_H [GHz]	7.47	7.39	7.39	7.22
	BW [GHz]	3.04	2.98	2.88	2.64
	FBW [%]	51.5	50.5	48.8	44.7
		WD	**ADS**	**WD**	**ADS**
		< –10 dB		< –10 dB	
$f_0 = 2.4$ GHz, $Z_1 = 50\ \Omega$, $Z_2 = 70.7\ \Omega$, $Z_{0e} = 189.25\ \Omega$, $Z_{0o} = 89.25\ \Omega$	f_L [GHz]	1.62	1.66	1.61	1.63
	f_H [GHz]	3.18	3.14	3.20	3.17
	BW [GHz]	1.56	1.48	1.59	1.54
	FBW [%]	65.0	61.7	66.3	64.2
		WD	**ADS**	**WD**	**ADS**
		< –15 dB		< –15 dB	
$f_0 = 2.4$ GHz, $Z_1 = 43.3\ \Omega$, $Z_2 = 86.7\ \Omega$, $Z_{0e} = 120\ \Omega$, $Z_{0o} = 20\ \Omega$	f_L [GHz]	1.88	1.86	2.04	2.00
	f_H [GHz]	2.92	2.94	2.77	2.80
	BW [GHz]	1.04	1.08	0.73	0.80
	FBW [%]	43.3	45.0	30.4	33.3

B. Branch-line Coupler – Case II

To further evaluate the robustness of the branch-line coupler structure shown in Fig. 9, stringent performance thresholds were applied to both the return loss (S_{11}) and isolation (S_{14}) characteristics across five distinct design configurations as shown in Table II. The versatility of the proposed coupled-line branch-line architecture is demonstrated through the simulation of various coupling coefficients, ranging from −10 dB to −30 dB at a design frequency of 10 GHz. Across all configurations, the return loss (S_{11}) and isolation (S_{14}) consistently exceed −30 dB and −40 dB, respectively, at the center frequency.

The comparative data between the WD modeling and ADS simulations reveals a consistent agreement in both absolute bandwidth and fractional bandwidth metrics.

Furthermore, the close correlation between the WD and ADS results for both f_L and f_H transition points reinforce the validity of the WD approach for modeling complex, multi-section microwave structures. The broadband nature of the design is evidenced by the characteristic dual-resonance behavior in the S_{11} magnitude plots, which ensures stable operation across a wide fractional bandwidth regardless of the specific coupling target. These results confirm that the impedance transformation properties of the Z_{03} and Z_{02} coupled-line sections are robust across a wide range of even- and odd-mode impedance values.

WD models are very good for understanding the theory and basic operation (equal/unequal power split, bandwidth), and are useful in early design stages. Therefore, they can be used for initial functional verification and *S*-parameter behavior evaluation.

TABLE II
RELIABILITY OF WD MODELS OF COUPLER CASE II
$f_0 = 10$ GHz, $Z_{03e} = 123\ \Omega$, AND $Z_{03o} = 40\ \Omega$

Branch-line coupler specifications		Return Loss S_{11}		Isolation S_{14}	
		WD	**ADS**	**WD**	**ADS**
		< –20 dB		< –25 dB	
$C = -10$ dB, $Z_1 = 33.5\ \Omega$, $Z_{02e} = 182\ \Omega$, $Z_{02o} = 42\ \Omega$	f_L [GHz]	7.52	7.45	8.45	7.35
	f_H [GHz]	12.48	12.55	11.55	12.65
	BW [GHz]	4.96	5.10	3.10	5.30
	FBW [%]	49.6	51.0	31.0	53.0
		WD	**ADS**	**WD**	**ADS**
		< –20 dB		< –30 dB	
$C = -15$ dB, $Z_1 = 34.5\ \Omega$, $Z_{02e} = 195\ \Omega$, $Z_{02o} = 65\ \Omega$	f_L [GHz]	7.82	7.50	7.90	7.25
	f_H [GHz]	12.18	12.50	12.10	12.75
	BW [GHz]	4.36	5.00	4.20	5.50
	FBW [%]	43.6	50.0	42.0	55.0
		WD	**ADS**	**WD**	**ADS**
		< –20 dB		< –40 dB	
$C = -20$ dB, $Z_1 = 34.5\ \Omega$, $Z_{02e} = 179\ \Omega$, $Z_{02o} = 88\ \Omega$	f_L [GHz]	7.95	7.55	8.33	7.60
	f_H [GHz]	12.05	12.45	11.68	12.40
	BW [GHz]	4.10	4.90	3.35	4.80
	FBW [%]	41.0	49.0	33.5	48.0
		WD	**ADS**	**WD**	**ADS**
		< –20 dB		< –40 dB	
$C = -25$ dB, $Z_1 = 34.5\ \Omega$, $Z_{02e} = 199\ \Omega$, $Z_{02o} = 120\ \Omega$	f_L [GHz]	7.98	7.60	7.73	7.30
	f_H [GHz]	12.03	12.40	12.28	12.70
	BW [GHz]	4.05	4.80	4.55	5.40
	FBW [%]	40.5	48.0	45.5	54.0
		WD	**ADS**	**WD**	**ADS**
		< –20 dB		< –40 dB	
$C = -30$ dB, $Z_1 = 34.5\ \Omega$, $Z_{02e} = 152.5\ \Omega$, $Z_{02o} = 120\ \Omega$	f_L [GHz]	7.98	7.60	7.23	6.90
	f_H [GHz]	12.03	12.40	12.78	13.10
	BW [GHz]	4.05	4.80	5.55	6.20
	FBW [%]	40.5	48.0	55.5	62.0

C. Discussion

The performance of the investigated branch-line couplers is validated using two distinct numerical paradigms: the industry-standard ADS frequency-domain solver and a custom-developed WD time-domain model. While both methods aim to characterize the scattering parameters (*S*-parameters) of the device, they differ fundamentally in their mathematical formulation and computational execution.

The ADS environment utilizes a frequency-domain approach, typically employing Method of Moments (MoM) or Harmonic Balance solvers. In this framework, the microwave structure is treated as a set of linear algebraic equations derived from Kirchhoff's laws and telegrapher's equations.

The solver computes the steady-state response of the network by sweeping through a range of frequencies. This method is highly optimized for extracting precise magnitude and phase information, particularly when accounting for complex microstrip dispersion and parasitic effects inherent in high-frequency coupled-line geometries. ADS shows what happens after the signal has reached a stable state. It doesn't inherently show you how the signal travels through the coupler in real-time.

Conversely, the WD approach is rooted in the DSP domain, where analog components are translated into discrete-time digital structures. The WD model utilizes incident and reflected wave variables rather than traditional voltages and currents. Each physical segment of the coupler, including the horizontal and vertical coupled-line sections, is modeled as a digital block with specific port resistances. In WD, the nodes in schematic are treated as "scattering matrices" (adaptors). The signal is literally scattered based on the impedance mismatches between the series and shunt branches.

As mentioned, the interconnection of these ports is managed via multi-port adaptors, which mathematically represent the junctions where power division and coupling occur. Unlike the static nature of frequency-domain sweeps, the WD model simulates the signal sample-by-sample, providing a native transient response. One can actually see the pulse travel from Port 1, split across the branches, and recombine at the output ports over time. The *S*-parameters are subsequently extracted by applying a Fast Fourier Transform (FFT) to the reflected and transmitted time-domain pulses.

The primary advantage of the WD approach in this research lies in its ability to simulate the coupler's behavior under modulated or pulsed signals, which is critical for modern telecommunications and IoT (Internet of Things) applications. However, numerical discrepancies observed at the band edges (below 6 GHz and above 14 GHz) can be attributed to the bilinear transformation used in WD modeling, which introduces frequency warping as the signal approaches the Nyquist limit of the simulation's sampling frequency.

By comparing the WD results against the ADS benchmark, we demonstrate that the WD model maintains a high degree of fidelity, typically within a 1% margin for fractional bandwidth, proving its efficacy as a computationally efficient tool for the rapid prototyping of wideband microwave components.

VI. Conclusion

This paper presented WD models for two wideband branch-line coupler configurations with open-circuited and open/short-circuited parallel-coupled sections. The models demonstrated FBW agreement within ~1% vs ADS for Case I, and within ~2–5% for most Case II configurations, confirming their validity for early-stage design verification.

To conclude, wave digital models offer a reliable and efficient method for simulating the frequency response of branch-line couplers. By discretizing the underlying analog structure into wave-based representations, these models maintain key properties such as passivity, causality, and numerical stability, which are essential for reliable RF simulations. Their modular nature facilitates the accurate modeling of distributed elements and complex topologies, enabling precise prediction of *S*-parameters across a wide frequency range. Consequently, wave digital modeling serves as a valuable technique for the design and optimization of high-frequency microwave components, including branch line couplers, within modern CAD (Computer-aided design) environments.

Acknowledgement

This work has been supported by the Ministry of Science, Technological Development and Innovation of the Republic of Serbia [Grant Number: 451-03-34/2026-03/200102].

References

[1] T. Jensen, V. Zhurbenko, V. Krozer, and P. Meincke, "Coupled Transmission Lines as Impedance Transformer", *IEEE Transactions on Microwave Theory and Techniques*, 2007, vol. 55, no. 12, pp. 2957-2965, DOI: 10.1109/TMTT.2007.909617

[2] Y. Haoka, T. Kawai and A. Enokihara, "Design of Broadband Branch-Line Couplers Utilizing Coupled Transmission Lines at Ka-Band", *2019 12th Global Symposium on Millimeter Waves (GSMM)*, Sendai, Japan, 2019, pp. 41-43, DOI: 10.1109/GSMM.2019.8797672

[3] R. K. Barik, S. Koziel and S. Szczepanski, "Wideband Highly-Selective Bandpass Filtering Branch-Line Coupler", *IEEE Access*, vol. 10, pp. 20832-20838, 2022, DOI: 10.1109/ACCESS.2022.3152802

[4] A. Fettweis, "Digital Circuits and Systems", *IEEE Trans. on Circuits and Systems*, vol. CAS-31, no. 1, Jan. 1984, pp. 31-48

[5] A. Fettweis, "Wave Digital Filters: Theory and Practice", *Proc. IEEE*, vol. 74, 1986, pp. 270-327

[6] S. Bilbao, *Wave and Scattering Methods for Numerical Simulation*, Wiley, Hoboken, New Jersey, 2004

[7] B. P. Stošić and N. S. Dončov, "Combined Wave Digital/Full-Wave Approach in Modeling and Analysis of Microstrip Structures with Examples in MATLAB/Simulink", Chapter 4 in *Advances in Engineering Research*, Nova Science Publishers, Inc., 2016, vol. 12, pp. 75-140

[8] P. Belforte, D. Spina, L. Lombardi, G. Antonini, T. Dhaene, "Automated Framework for Time-domain Piecewise-linear Fitting Method based on Digital Wave Processing of S-Parameters", *IEEE Trans. on Circuits and Systems I: Regular Papers*, 2019, pp. 1-14, DOI: 10.1109/TCSI.2019.2944198

[9] P. Belforte and G. Guaschino, *DWS 9.0 Digital Wave Simulator*, User's Manual, Jan. 2020, DOI: 10.13140/RG.2.2.11489.66407/1

[10] P. Belforte, D. Spina, G. Antonini, L. Lombardi, and T. Dhaene, "Time-domain Piecewise-linear Fitting Method based on Digital Wave Processing of S-parameters", DOI: 10.13140/RG.2.2.34124.36481/2

[11] P. Belforte, D. Spina, M.D. Astorino, G. Antonini, M. Ferrar, "Frequency Domain Behavior of S-parameters Piecewise-linear Fitting in a Digital-wave Framework", *Intern. Journal of Numerical Modelling*, 2022, vol. 35, no. 1, e2934, DOI: 10.1002/jnm.2934

[12] A. Bernardini, E. Bozzo, F. Fontana, and A. Sarti, "A Wave Digital Newton-Raphson Method for Virtual Analog Modeling of Audio Circuits with Multiple One-port Nonlinearities", *IEEE/ACM Transactions on Audio, Speech, and Language Processing*, DOI: 10.1109/TASLP.2021.3084337

[13] B. P. Stošić, M. Nedelchev, and P. Belforte, "Wave Digital Frameworks for Simulation of Microwave Couplers: Transmission Line Versus Equivalent Lumped Circuit", *2021 15th International Conference on Advanced Technologies, Systems and Services in Telecommunications (TELSIKS)*, Serbia, Niš, October 20-22, 2021, pp. 175-178, DOI: 10.1109/TELSIKS52058.2021.9606374

[14] B. P. Stošić, "Wave-based Digital Models of Different Branch-line Couplers", *Serbian Journal of Electrical Engineering*, vol. 17, no. 2, June 2020, pp. 149-169, DOI: 10.2298/SJEE2002149S

[15] B. P. Stošić, M. Nedelchev, and Z. Marinković, "Modular Wave Digital Approach: Methodology Review and Application on Wilkinson-type Power Dividers", *Cogent Engineering*, vol. 12, no. 1, 2025, DOI: 10.1080/23311916.2025.2573877

[16] D. M. Pozar, *Microwave Engineering*, Wiley, 4th Edition, 2011

[17] G. Matthaei, L. Young, and E.M.T. Jones, *Microwave Filters, Impedance-Matching Networks, and Coupling Structures*, Artech House, Inc., Dedham, Massachusetts, 1980

[18] B. P. Stošić and N. Dončov, "Synthesis and Use of Wave Digital Networks of Admittance Inverters", *Microwave Review*, vol. 19, no. 2, December 2013

[19] B. P. Stošić, "Wave Digital Network of Parallel-coupled Microstrip based on Admittance Inverter Model", *2013 11th International Conference on Telecommunications in Modern Cable, Satellite and Broadcasting Services (TELSIKS)*, Serbia, Niš, October 16-19, 2013, vol. 1, pp. 249-252, DOI: 10.1109/TELSKS.2013.6704927

[20] L. K. Yeung and K.-L. Wu, "A Dual-Band Coupled-Line Balun Filter," in *IEEE Transactions on Microwave Theory and Techniques*, vol. 55, no. 11, pp. 2406-2411, Nov. 2007, DOI: 10.1109/TMTT.2007.907402

[21] M. Makimoto and S. Yamashita, "Bandpass Filters Using Parallel Coupled Strip-Line Stepped Impedance Resonators," *1980 IEEE MTT-S International Microwave Symposium Digest*, Washington, DC, USA, 1980, pp. 141-143, DOI: 10.1109/MWSYM.1980.1124210

[22] W. A. Arriola, J. Y. Lee and I. S. Kim, "Wideband 3 dB Branch Line Coupler Based on λ/4 Open Circuited Coupled Lines", *IEEE Microwave and Wireless Components Letters*, vol. 21, no. 9, pp. 486-488, Sept. 2011, DOI: 10.1109/LMWC.2011.2138687

[23] B. P. Stošić and M. Nedelchev, "Reliability of the Digital Model of an Open-Circuited Coupled-Line Branch-Line Structure," *60th International Scientific Conference on Information, Communication and Energy Systems and Technologies (ICEST)*, Ohrid, North Macedonia, 2025, pp. 1-4, DOI: 10.1109/ICEST66328.2025.11098325

[24] L. Wanhammar and T. Saramaki, *Digital Filter using MATLAB*, Springer Nature Switzerland AG, 2020

[25] Y. Haoka, T. Kawai, and A. Enokihara, "Design of Broadband Branch-Line Couplers Utilizing Coupled Transmission Lines at Ka-Band", *2019 12th Global Symposium on Millimeter Waves (GSMM)*, Sendai, Japan, 2019, pp. 41-43, DOI: 10.1109/GSMM.2019.8797672